J Mater Sci (2008) 43:6676–6681
DOI 10.1007/s10853-008-2801-0



# Preform permeability variation with porosity of fiberglass and carbon mats

**Hossein Golestanian**

Received: 15 April 2008 / Accepted: 11 June 2008 / Published online: 31 July 2008


**Abstract** An experimental investigation on fiber bed permeability variation with porosity for three types of reinforcement mats is performed. The reinforcements consist of plain-weave carbon, plain-weave fiberglass, and chopped fiberglass mats. Resin flow experiments are performed in a rectangular cavity with different fiber volume fractions. RL 440 epoxy resin is used as the working fluid in the experiments. Several layers of mats are laid inside the mold in each experiment and resin is injected at a constant pressure. The effects of reinforcement type and porosity on fiber bed permeability are investigated. Fiber mat permeability of woven mats show large degrees of anisotropy. Resin flow in chopped fiberglass mats is circular, suggesting an isotropic permeability tensor. In all the three cases, preform permeability increases with fiber bed porosity in a non-linear fashion. The results of this investigation could be employed in optimization of liquid composite molding manufacturing processes.

## Nomenclature

| | |
|---|---|
| $Aw$ | Total weight of a fabric ply |
| $d_f$ | Fiber density |
| $K$ | Isotropic permeability |
| $K$ | Directional permeability in the direction of maximum flow |
| $K_2$ | directional permeability in the direction of minimum flow |
| $m$ | Slope of the best fit line |
| $N$ | Number of plies |
| $R_f$ | Radius of the moving fluid |
| $R_o$ | Radius of the injection port |
| $t$ | Time |
| $T_m$ | Thickness of the laminated fabric preform |
| $v$ | Fluid velocity |

### Greek symbols

| | |
|---|---|
| $\alpha$ | Ratio of the permeabilities |
| $\varepsilon$ | Porosity of the fiber bed |
| $\eta$ | Elliptical equivalent of the in-plane angle |
| $\Phi$ | Function based on the maximum in-plane permeability |
| $\mu$ | Fluid viscosity |
| $\Delta P$ | Pressure gradient |
| $\rho$ | Fluid density |
| $\rho_f = R_f/R_o$ | Dimensionless radial extent |
| $\xi_o$ | Elliptical equivalent of the injection port radius |
| $\xi_f$ | An elliptical extent |

## Introduction

Fiber bed permeability is an important process parameter in the manufacturing of composite parts. This parameter must be determined experimentally for every fiber type and volume fraction prior to process/tool design. For example, in Resin Transfer Molding (RTM), resin flow behavior determines the integrity of the manufactured composite part. The injection cycle must be planned very carefully to ensure the production of a defect-free part. This optimization must be performed in the mold design phase of the production planning to reduce trial and error costs. The main process parameters include injection port position, injection pressure, resin viscosity, and injection time.

H. Golestanian (✉)
Mechanical Engineering Department, University of Shahrekord, Kilometer 2 of Saman Road, Shahrekord, Iran
e-mail: golestanian@eng.sku.ac.ir

These parameters could be determined only when the fiber bed permeability is known. RTM is a process which involves the injection of liquid resin into an enclosed mold containing previously positioned reinforcement preforms. This process can be employed to manufacture large and complicated composite parts. Typical examples of products that are produced with RTM include parts in automotive and aircraft industries, fiberglass boats, swimming pools, and bathtubs [1, 2]. The reinforcement is composed of several layers of chopped or woven fiber mats laid inside a two-piece mold. The mold is closed and resin is injected into the mold through one or multiple injection ports to impregnate the fibers of the preform. Injection time depends on the size of the part, fiber volume fraction, fiber type, resin viscosity, and injection pressure. Once the mold is completely filled, injection is stopped and the part is cured inside the mold. Mold design is a highly labor intensive and complex operation [2]. Proper mold filling requires proper positioning of the inlets and outlets, close monitoring of mold temperature, and selection of optimum injection pressure [3]. Injection time must be long enough to ensure complete preform impregnation.

Therefore, fiber mat permeability determination is an important step in mold design and process control in an RTM process. In determination of the required injection time and pressure, one needs to determine this parameter in advance. This fiber bed property depends on the amount of voids and their orientation within the fiber bed assembly. Thus, the main factors affecting permeability are the type of fiber mat, the preform porosity, and the fiber volume fraction inside the mold.

## Literature survey

Many investigators have performed research on permeability determination and resin flow analysis in RTM processes in the past decades. Golestanian et al. [2, 3] have modeled resin flow and cure of rectangular and irregular composite parts. They conducted experiments to determine fiber mat permeability for 5-harness carbon and 8-harness glass mats. They determined these properties assuming that fiber beds were homogeneous. These investigators performed experiments only on a single fiber volume fraction preform and did not investigate the effects of fiber bed porosity on permeability. Perry et al. [4] performed permeability measurements on woven graphite fibers. They considered a two-dimensional mold filling case. Parnas et al. [5] performed experimental and theoretical analyses to determine flow behavior in porous media. They investigated flow in heterogeneous reinforcement structures and the possibilities of void formation as a result. By performing one-dimensional flow measurement experiments, they determined the permeability for several types of woven mats. Choi et al. [6] used a finite element software package to determine the permeability at a microscopic level. They then developed a flow model to predict resin flow in real fiber preforms. Their model predicts the interrelationship between preform properties such as permeability, fiber packing, fiber radius, and fiber volume fraction. Sawley et al. [7] used smooth particle hydrodynamics in finite element models to predict the flow through porous media. They modeled the porous media as a network of particles between which fluid flow occurred. They performed experimental measurements and compared the results with their numerical results. They demonstrated that Darcy's law predicts flow accurately when the drift velocity is low. Lam et al. [8] used finite element method to simulate mold filling in rectangular and semi-cylindrical composite parts. They considered one-dimensional resin flow and did not present any experimental verification of their results. Lim and Lee [9] simulated mold filling of thick rectangular composite parts. They determined three-dimensional permeability tensor for glass fiber mats. These investigators compared their flow analysis results with experimental measurements and found up to 32% error in resin front positions in some places inside the domain. These researchers also performed flow analysis in manufacturing of a centrifugal pump cover. Han et al. [10] performed permeability measurements of anisotropic fiber preforms with a higher fiber content. These investigators performed pressure measurements at four locations in the flow field to determine the permeabilities for several types of fiber preforms. Babu and Pillai [11] performed experiments on resin flow behavior into woven, stitched, and braided fiber mats. They used a rectangular flat mold with a resin-like fluid for their experiments. They investigated inlet pressure drop with time and did not present any resin velocity data. Luka et al. [12] performed a draping analysis for the determination of fiber mat permeability as a function of deformation. They then used their determined permeability values in numerical models for the flow analysis of a car bonnet. Adams and Rebenfeld [13, 14] performed theoretical and experimental investigations on fiber mat permeability of anisotropic fiber preforms. They performed experiments on non-woven polyester and woven Kevlar fabric to determine permeability of these fibers. They also investigated the effects of the number of fiber mats on permeability of multilayer fiber assembly. By changing the sequence of low and high permeability layers, they enhanced the permeability of fiber assembly. Ahn and Seferis [15] investigated the applicability of Kozeny–Carman equation to determine the permeability of fiber beds in composite manufacturing. They performed measurements on plain-weave T-300 carbon fabric. Their results suggested a linear increase in the permeability with fiber preform porosity.

All of the above investigators modeled resin flow inside the mold as a flow through porous media and employed Darcy's law in their analyses. Few have determined fiber mat permeability experimentally. Fiber mat permeabilities have not been determined experimentally for plain-weave fiberglass, plain-weave carbon, and chopped fiberglass assemblies with different porosity values. The author is the first to determine the permeability variation with porosity for the three fiber types mentioned above.

## Flow measurement experiments

A series of flow measurement experiments were designed to simulate the mold filling stage of an RTM process. A rectangular mold was designed and built from Plexiglas for this purpose. This mold consisted of two flat plates of Plexiglas approximately 28 × 18 × 1.0 cm. A 24 × 14 cm cavity was cut inside a 0.3-cm-thick Plexiglas plate to be used as a spacer between the top and bottom pieces of the mold. This cavity represented the rectangular mold. A series of screws were used to put the three pieces together.

The experimental setup consisted of an air pump which supplied pressurized air to a pressure regulator. The injection pressure can be adjusted to the desired level and kept constant using this regulator. The resin is put into a reservoir connected to the pressure regulator using a piece of plastic tubing. Resin enters the mold cavity through a central injection port devised on the top plate. A stop watch is used to keep track of the elapsed time. The mold is placed on top of a 0.5-cm-thick clear safety glass in a four-legged fixture made of dextron. Two mirrors, placed at 45-degree angle in the fixture, are used to reflect the top and bottom views of the mold. The safety glass was leveled so that the flow would be induced only by the air pressure and not by the gravitational force. A video camera, facing the mirrors, is used to record resin flow behavior in the mold.

RL 440 epoxy resin was used in the flow simulation experiments as the working fluid and all experiments were performed under constant injection pressure. Several flow measurements were performed with each combination of fiber type, preform porosity, and injection pressure. Experiments on chopped fiberglass mats were performed under injection pressures ranging from 43.0 to 96.0 kPa. With these pressures, the rectangular mold filled at 300–800 s. Injection pressures were varied between 62.4 and 86.2 kPa and fill times of 250–800 s were recorded for woven fiberglass mats. For the same geometry and injection pressures between 64.6 and 79.7 kPa, fill times were between 1,000 and 1,600 s for the carbon fiber mats. A comparison between the required injection times can be made between woven fiberglass and carbon fiber mats as the experiments were performed with close fiber bed porosity values. It is noted that required injection time is much higher for carbon fiber mats as will be explained in the results section.

A total of 25 experiments were performed with woven fiberglass mats. Preform porosity was varied between 0.51 and 0.74 in these experiments. The number of experiments performed on the chopped fiberglass mats was 15. For this type of mat, porosity values in the range of 0.72 to 0.84 were used. In addition, 11 experiments were performed with woven carbon fiber mats with porosity values ranging from 0.44 to 0.56. From the experiments on each fiber type, several were selected for data analysis. The selection was made based on how well resin flow behaved during the injection cycle. Most of the experiments were satisfactory, but in some cases, resin flow behaved in an unexpected manner. In some cases, flow channeling was observed, and in some experiments, air was trapped inside the mold in which case resin flow became too slow. These cases were marked as "bad" experiments and were eliminated from data analysis. Data analysis procedures and experimental results are presented in the next section.

## Analysis

As mentioned earlier, every experiment was videotaped. Next, frames from these tapes were frozen and printed at certain time intervals and measurements were performed on these frames. Based on the type of the fiber mat, two types of flow were observed. Resin flow in chopped fiberglass mats was circular, suggesting an isotropic permeability. In the case of woven fiberglass and woven carbon fiber assemblies, resin front had an elliptic shape. This elliptic flow front suggests an orthotropic preform [13]. Analysis in each case was then performed based on the resin front shape observed in these experiments. Formulations and analytic procedures for these cases are described below.

### Analysis of isotropic preform

The isotropic working equation for the in-plane flow experiment is [3],

$$\frac{dR_f}{dt} = \frac{K\Delta P}{\varepsilon\mu}\frac{-1}{R_f \ln\left(R_f/R_o\right)} \tag{1}$$

where $R_f$ and $R_o$ are the radii of the moving fluid and the injection port, respectively. The boundary condition for Eq. (1) is, $R_f = R_o$ at $t = 0$.

The solution for Eq. (1) subject to the above boundary condition is [3],

$$G(\rho_f) = [\rho_f^2(2\ln\rho_f - 1) + 1]/4 = \frac{K\Delta P t}{\varepsilon\mu R_o^2} \quad (2)$$

where $\rho_f = R_f/R_o$ is the dimensionless radial extent. In Eq. (2), $\Delta P$ is specified experimentally and $\varepsilon$ is known from the fibrous preform type and number of lamina. Discrete $R_f(t)$ data may be plotted in the form of $G(\rho_f)$ vs. time as suggested by Eq. (2). Least square line is fit through the data, and the isotropic in-plane permeability is determined from the slope of the line as [3]

$$K = \frac{m\varepsilon\mu R_o^2}{\Delta P} \quad (3)$$

where $m$ is the slope of the best fit line through the data. The porosity of the stacked fiber mat layers is given by [16]

$$\varepsilon = 1 - \frac{NA_w}{\rho_f T_m} \quad (4)$$

In Eq. (4), $N$ is the number of plies, $A_w$ is the total weight of a fabric ply, $d_f$ is fiber density, and $T_m$ is the thickness of the laminated fabric preform.

The analysis involves resin front measurements with time during the injection cycle. Thus, resin front positions were measured from the printed frames and the degree of circularity was checked. For chopped fiberglass mats, which were isotropic, the results were plotted as $G(\rho_f)$ vs. time and the best fit line was obtained. Using the slope of the best fit line in Eq. (3), the permeability was determined for three preform porosity values. The results of these analyses are presented in the Experimental Results section.

## Analysis of orthotropic preform

Resin front advanced with an elliptic shape in the experiments with woven fiberglass and woven carbon fiber mats. This suggests an orthotropic permeability tensor for these mats. The analysis in this case follows the formulation given by Adams and Rebenfeld [13, 14]. In this case, the governing differential equation of the moving resin front is,

$$\frac{d\zeta}{dt} = \frac{k_1\Delta P}{\varepsilon\mu R_o^2}\left[\frac{\alpha}{1-\alpha}\right]\left[\frac{1}{(\zeta_f - \zeta_o)(\cosh^2\zeta_f - \cos^2\eta)}\right] \quad (5)$$

In Eq. (5), $\xi_f$ is an elliptical extent, $\eta$ is the elliptical equivalent of the in-plane angle, and $\alpha$ is the ratio of the permeabilities, which is given by

$$\alpha = \frac{K_2}{K_1} \quad (6)$$

where $K_1$ and $K_2$ are the directional permeabilities in the directions of maximum and minimum resin flow, respectively.

In addition, $\xi_o$ is the elliptical equivalent of the injection port radius given by,

$$\zeta_o = \ln\left[\frac{1+\alpha^{1/2}}{(1-\alpha)^{1/2}}\right] \quad (7)$$

Subjected to the initial conditions, $\xi_f = \xi_o$ at $t = 0$.

The relations between the radial and elliptical extents in these directions are given by;

$$\zeta_{f1} = \sinh^{-1}\left[\frac{R_{f1}}{R_o}\left(\frac{1}{\alpha} - 1\right)^{-1/2}\right] \quad (8)$$

and

$$\zeta_{f2} = \cosh^{-1}\left[\frac{R_{f2}}{R_o}(1-\alpha)^{-1/2}\right] \quad (9)$$

The solution to Eq. (5) is

$$F(\zeta_f,\eta) = (\zeta_f - \zeta_o)\left(\frac{\sinh(2\zeta_f)}{4} + \frac{\zeta_f}{2}\right) + \cos^2\eta(\zeta_f\zeta_o - (\zeta_f^2 + \zeta_o^2)/2) + (\cosh(2\zeta_o) - \cosh(2\zeta_f))/8 + (\zeta_o^2 - \zeta_f^2)/4 = \left[\frac{\alpha}{1-\alpha}\right]\Phi \quad (10)$$

where $\Phi$ is based on the maximum in-plane permeability $K_1$.

The orthotropic data analysis is iterative in $\alpha$. First, $\alpha$ is guessed and the experimental data are converted to equivalent elliptical extents and are plotted for the two datasets. A single least square analysis is then performed on the two sets of data. The single least square line will not fit both sets of data properly if $\alpha$ is not chosen correctly. By changing $\alpha$ and monitoring the errors, the best value for $\alpha$ is selected. After $\alpha$ is selected properly, the slope of the best fit line is used in Eq. (11) below, along with Eq. (6) to determine the directional permeability values, $K_1$ and $K_2$.

$$m_\zeta = \frac{K_1\Delta P}{\varepsilon\mu R_o^2}\left[\frac{\alpha}{1-\alpha}\right] \quad (11)$$

## Results and discussion

Analyses were performed based on the experimental results of the three types of fiber mats following the procedures outlined above. The results of the best fit lines are presented for the selected experiments with each fiber mat type in Figs. 1–3. In case of chopped fiberglass mats, the analysis followed the isotropic analysis procedure. The best fit line for the selected experiment on these mats is presented in Fig. 1. Note that one set of data points is measured and fitted since circular flow patterns were observed in the chopped fiberglass mats. Figure 2 presents the results of the selected experiment on woven fiberglass mats. The flow pattern was elliptic in this case and two sets of data points are fitted by a single best fit line as explained in the analysis section. The results of the selected

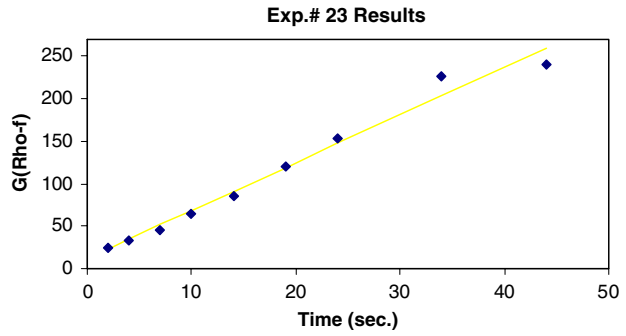


**Fig. 1** The best fit line fitted through the experimental data on chopped fiberglass mats

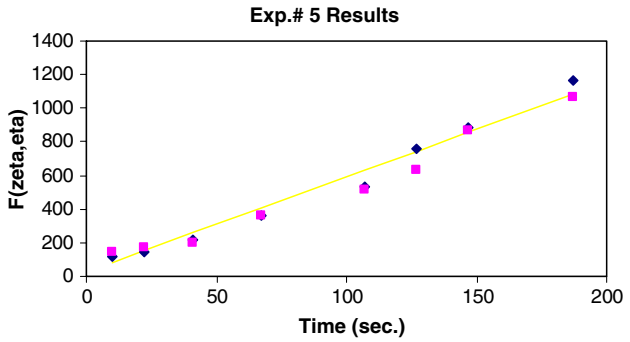


**Fig. 2** The best fit line fitted through the experimental results on woven fiberglass mats

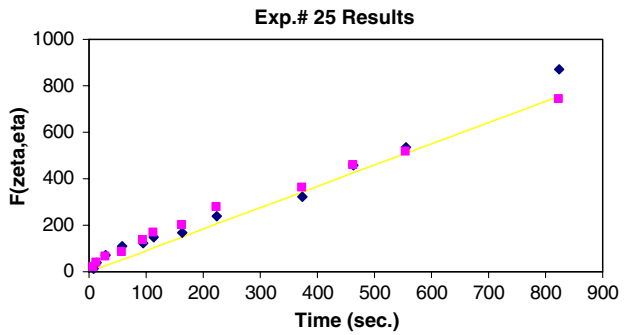


**Fig. 3** The best fit line fitted through the experimental results on woven carbon mats

experiment on woven carbon fiber mats are shown in Fig. 3. The analysis followed the orthotropic preform procedure for the carbon mats as well.

The analysis was performed on several cases for each fiber type. In each case, the effect of fiber bed porosity on permeability was investigated. From the results of these analyses, plots of permeability vs. porosity were generated for each fiber type. Resin viscosity was taken as 440 centipoises. Figure 4 depicts the variation of fiber bed permeability with porosity for chopped fiberglass mats. The results indicate an increase in permeability with

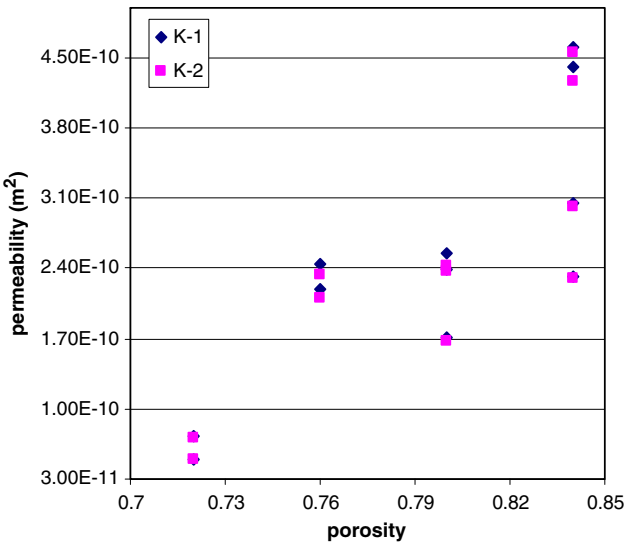


**Fig. 4** Variation of fiber bed permeability with porosity for chopped fiberglass mats

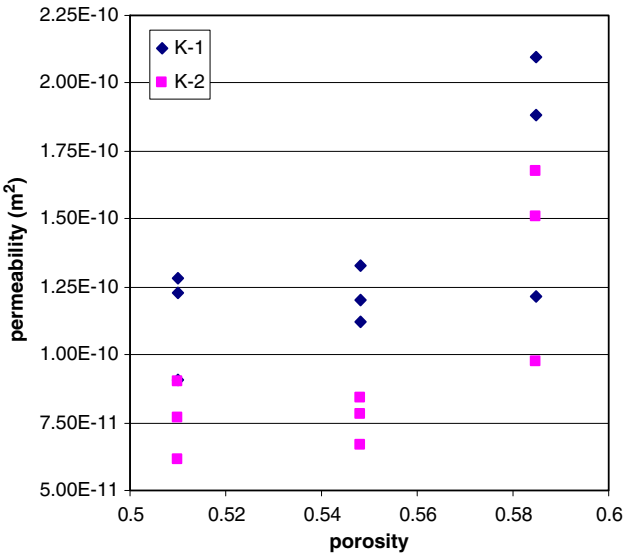


**Fig. 5** Variation of fiber bed permeability with porosity for woven fiberglass mats

increasing porosity. Also, note that permeability increases sharply as porosity increases from 0.8 to 0.84. This suggests that, at high porosity values, resin flows more easily into the preform since more voids are present within the mats inside the mold cavity. This suggests longer injection time for parts with higher fiber content and lower preform porosity.

Variation of permeability with porosity for woven fiberglass mats is shown in Fig. 5. Again an increase in permeability is observed with fiber bed porosity, especially as porosity increases above 0.55. Also, note that this fiber preform is anisotropic and values of $K_1$ are larger than that of $K_2$ at all porosity values. Resin front advanced in an elliptic manner in woven glass preform.

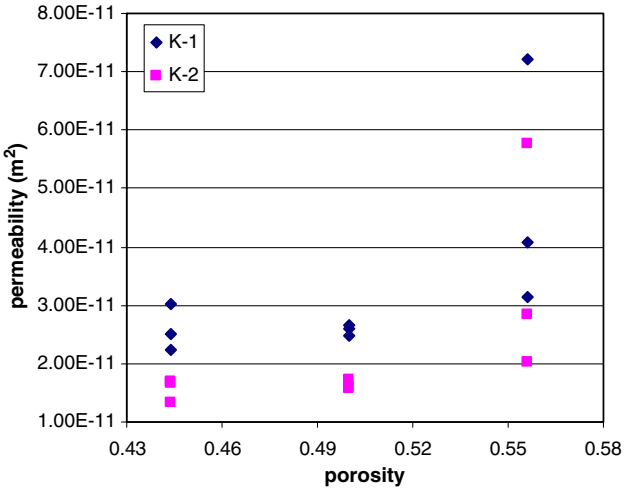


**Fig. 6** Variation of fiber bed permeability with porosity for woven carbon mats

The case of woven carbon fiber mats is shown in Fig. 6. Permeability increases with porosity for this reinforcement type as well. Also, permeability tensor is anisotropic for the woven carbon mats. In addition, at equal porosity values, carbon mat permeability is more than three times smaller than that of woven fiberglass mats. This suggests that, at constant fiber volume fractions, longer injection time is expected in the manufacturing of composite parts with carbon mats.

## Concluding remarks

Resin flow experiments were performed to determine variation of fiber bed permeability with preform porosity. Three types of fiber preforms were used in the experiment. The investigation was performed with woven carbon mats, woven fiberglass mats, and chopped fiberglass mats. Experiments were performed at three fiber bed porosity values with each fiber type. Each experiment was performed under constant pressure conditions and RL 440 epoxy resin was used as the working fluid. Permeability tensor for chopped fiberglass mats was found to be isotropic. In case of woven fiberglass and woven carbon mats, permeability tensor came out to be orthotropic. That is, resin flow in these mats was elliptic. In general, preform permeability increases sharply as porosity increases above a certain value. This suggests a decrease in permeability with an increase in fiber volume content. This means higher injection times and, in turn, higher manufacturing costs for a part with higher fiber content in an RTM process. In addition, fiber bed permeability was measured to be much lower for carbon mats. This indicates that the injection cycle will be several times larger for parts manufactured using carbon fiber mats in comparison with either chopped or woven fiberglass mats with the same porosity or fiber content.

## References

1. Richardson T (1987) Composites a Design Guide. Industrial Press Inc., New York
2. Golestanian H (1997) PhD thesis, University of Missouri, Columbia, MO
3. Golestanian H, El-Gizawy Sherif A (1998) J Polym Compos 19(4):395
4. Perry MJ et al (1992) 24th International SAMPE Technical Conference, p T421
5. Parnas RS et al (1994) Compos Struct 27:93
6. Choi MA et al (1998) J Non-Newtonian Fluid Mech 79:585
7. Sawley ML et al (1999) CSIRO. Melbourne, Australia
8. Lam YC et al (2000) Compos Sci Technol 60:845
9. Lim ST, Lee WII (2000) Compos Sci Technol 60:961
10. Han KK (2000) Compos Sci Technol 60:2435
11. Babu BZ, Pillai KM (2002) SAMPE conference. Long Beach, CA
12. Luca P et al (2002) SAMPE conference. Long Beach, CA
13. Adams KL, Rebenfeld L (1991) Polym Compos 12(3):186
14. Adams KL, Rebenfeld L (1991) Polym Compos 12(3):179
15. Ahn KJ, Seferis JC (1991) Polym Compos 12(3):146
16. Bird RB, Stewart WE, Lightfoot EN (1960) Transport phenomena. Wiley, New York